IL NUOVO CIMENTO Vol. 35 C, N. 4 Luglio-Agosto 2012
DOI 10.1393/ncc/i2012-11271-0

Colloquia: PAVI11

A next generation measurement of the electric dipole moment of the neutron at the FRM II

I. Altarev(1), D. H. Beck(2), S. Chesnevskaya(1), T. Chupp(3), W. Feldmeier(1), P. Fierlinger(1), A. Frei(4), E. Gutsmiedl(1), F. Kuchler(1), P. Link(4), T. Lins(1), M. Marino(1), J. McAndrew(1), S. Paul(1), G. Petzoldt(1), A. Pichlmaier(4), R. Stoepler(1), S. Stuiber(1) and B. Taubenheim(1)

(1) *Physikdepartment Technische Universität München and Excellence-Cluster "Universe" Germany*
(2) *University of Illinois at Urbana-Champaign, Department of Physics Urbana, IL 61801, USA*
(3) *University of Michigan, Randall Laboratory - Ann Arbor, MI 48109, USA*
(4) *Technische Universität München, Forschungsneutronenquelle Heinz Maier-Leibnitz Germany*

ricevuto il 14 Ottobre 2011; approvato il 5 Maggio 2012
pubblicato online il 26 Giugno 2012

Summary. — In this paper we discuss theoretical motivations and the status of experimental searches to find time-reversal symmetry-violating electric dipole moments (EDM). Emphasis is given to a next generation search for the EDM of the neutron, which is currently being set up at the FRM II neutron source in Garching, with an ultimate sensitivity goal of 5×10^{-28} cm (3σ). The layout of the apparatus allows for the detailed investigation of systematic effects by combining various means of magnetic field control and polarized UCN optics. All major components of the installations are portable and can be installed at the strongest available UCN beam.

PACS 21.10.Ky – Electromagnetic moments.
PACS 24.80.+y – Nuclear tests of fundamental interactions and symmetries.
PACS 11.30.Cp – Lorentz and Poincaré invariance.
PACS 11.30.Er – Charge conjugation, parity, time reversal, and other discrete symmetries.

1. – Introduction

A non-zero value of an electric dipole moment (EDM) [1] of a fundamental system would represent a manifestation of yet unknown time reversal symmetry (T) violation. Assuming the conservation of the combined operation of CPT, T violation in a fundamental system also violates CP [2,3]. Only few experiments could provide data on this

TABLE I. – *Predicted EDM values and measured upper limits for different systems.*

System	Predicted EDM (ecm)	Measured (ecm)
Neutron	$\sim 10^{-32\pm1}$(SM) $\sim 10^{-26}$–10^{-28} (SUSY)	$d_n < 2.9 \cdot 10^{-26}$(90%) [13]
Electron	$\sim< 10^{-38}$(SM)	$d_e < 1.05 \cdot 10^{-27}$(90%) [14]
Nuclear EDM: ^{199}Hg	$\sim 10^{-33}$–10^{-34}(SM)	$d_{Hg} < 3.1 \cdot 10^{-29}$(95%) [15]

phenomenon which can be observed in Weak Decays involving quarks [3,4], as described by the Cabbibo-Kobayashi-Maskawa (CKM) matrix [5]. However, there are many open questions remaining. In this context, the measurement of an EDM is considered one of the most important experiments in this field [6]. Electric dipole moments of baryonic systems can be also used to search for the CP violating product of the gluon operators G and $\tilde{\mathrm{G}}$ in the QCD Lagrangian. This term is weighted with the parameter θ, which is already strongly restricted by measurements to $\theta < 10^{-10}$ [7] and is considered unnaturally small and called the strong CP problem. Measured CP violation also does not accommodate for the observed ratio of baryons to photons, related to the ratio of baryons to anti-baryons in Baryogenesis models [8], by ~ 9 orders of magnitude. It was pointed out by Sakharov [9] that, assuming the conservation of CPT, the explanation requires next to baryon number violation and departure from thermal equilibrium also additional sources of CP violation. A prominent example for an EDM search is the neutron, but also nuclei or electrons can have permanent electric dipoles [10]. The size of EDMs is predicted by the electroweak SM based on contributions of three loop level and is thus very small, *e.g.* for neutron this is on the order of $d_n \sim 10^{-32}$ ecm [11]. Supersymmetry (SUSY) and most other possible extensions of the SM give rise to larger values of EDMs, as they arise already at one loop level (*e.g.*, ref. [12]). Neutrons are favored systems due to their comparably simple composition and due to the possibility to actually perform extremely precise measurements. Table I shows the predicted and measured values for an EDM of selected systems.

The Hamiltonian of such a system is

$$\hbar\omega = -\frac{\vec{S}}{|S|}\left(\mu\vec{B} - d\vec{E}\right), \tag{1}$$

with μ the magnetic moment and d the electric dipole moment. The EDM is extracted by sequentially measuring the Larmor precession ω. A phase $\Delta\omega$ between measurements with parallel and anti-parallel orientations of $\vec{B}$ and $\vec{E}$ corresponds to the EDM:

$$d = \frac{\hbar\Delta\omega}{4E}\,. \tag{2}$$

Most neutron EDM experiments deploy trapped ultra-cold neutrons (UCN) and Ramsey's method of separated oscillating fields, effectively forming an interferometer in time: polarized UCN start out aligned parallel to a constant magnetic field B_0. A stable clock is operated outside the apparatus. An oscillating field B_1 aligned normal to B_0 referenced to the external clock rotates the spin into a plane normal to B_0. While the oscillator keeps running, the spin precesses freely for a time T with an additional E-field aligned either parallel or anti-parallel to B_0. After a second coherent $\pi/2$-pulse, the polarization is rotated back from the precession plane into the direction of B_0. The phase caused by

the electric field is then analyzed. In many cases a field of $B_0 \sim 1\,\mu$T ($\omega_L \sim 30\,$Hz) is chosen. The statistical accuracy of an EDM measurement is then

$$\sigma_d = \frac{\hbar}{2\alpha ET\sqrt{N}\sqrt{M}}\,, \tag{3}$$

where N is number of detected neutrons, α is a "quality" parameter for the measurement, including the polarization loss during the precession time T. A factor of $1/\sqrt{M}$ is added to the sensitivity formula with M the number of measurements. Currently, several collaborations worldwide try to measure EDMs with next generation approaches to achieve an improvement of the current limits by almost 2 orders of magnitude to the $10^{-28}\,$ecm regime, *e.g.* the Sussex-RAL-Oxford-Kure collaboration and the US community at the Spallation Neutron Source, who are building cryogenic experiments based on super-fluid ^{4}He for production and storage of UCN with very innovative approaches. Other groups at ILL and PSI use trapped UCN in vacuum at room temperature, their gain in sensitivity relies on the stepwise improvement of existing apparatus and technology. Although all these measurements are much less accurate than measurements of atomic systems, it is worthwhile to perform these measurements due to their strong impact on theory.

2. – The experiment

At the new source of UCN at the FRM-2 in Garching a next generation approach to measure the EDM of the neutron is currently being set up. It extends proven and already known technologies with the goal to achieve a statistical limit of $d_n < 5 \cdot 10^{-28}\,$ecm at 3σ and a corresponding control of systematic effects of $\sigma_{d,\mathrm{syst}} < 2 \cdot 10^{-28}\,$ecm ($1\sigma$). The main improvements are i) a strong source of UCN, ii) sufficient control of magnetic and electric fields and iii) improved possibilities to test for systematic effects. The source of UCN is placed in a tangential beam tube inside the reactor in a thermal neutron flux of $1 \cdot 10^{14}\,\mathrm{s}^{-1}$. Solid deuterium is used as a super-thermal converter for the production of UCN. Properties of the source and its operation could be tested previously [16-18]. Operation of the source at the reactor is expected in 2013. The UCN are extracted from the source and guided in vacuum to the experiments. A beam line made from specially prepared replica foil tubes with a relative transmission of > 0.99 per meter guides the UCN to the nEDM beam position, which is placed outside the reactor building in a new experiment hall at 27 m distance from the solid deuterium source. Taking into account production, volumes and losses of all components and the EDM chambers, the projected polarized UCN density is $> 3000\,\mathrm{cm}^{-3}$ in the EDM experiment.

Chosen from a finite number of possible realizations of a next generation measurement that have been discussed in the community over the last decades, this approach is based on UCN stored in two vertically aligned cylindrical vessels at room temperature and a vertical magnetic field B_0. In between the cells a high voltage electrode is placed to enable measurements with an electric field parallel and anti-parallel to B_0 simultaneously. Using the statistical sensitivity formula (eq. (3)) with practically feasible numbers for α, a precession time of $T = 250\,$s, an electric field $E = 18\,$kV/cm and the neutron number based on chamber dimensions of 12 cm height and 48 cm diameter, the statistical sensitivity goal can be achieved in 200 days. In addition, a co-magnetometer based on polarized ^{199}Hg vapor with a laser based optical system is placed in these cells [19], also allowing for light-shift free operation. External magnetometers are placed on top and bottom of the chambers inside tubes that are accessible from outside during operation of the experiment. A cut through the apparatus is shown in fig. 1. Buffer gases can be added

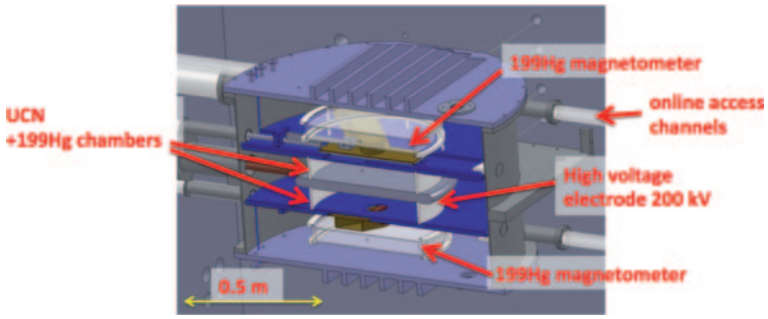

Fig. 1. – EDM measurement chamber stack with HV electrode, magnetometer cells on top and bottom and access tubes for additional magnetometry.

to all magnetometers to investigate various systematic effects and to eventually increase the HV behavior. Within close distance tangentially to the magnetometer cells, tubes are placed that reach through the vacuum chamber and can be accessed from outside during the measurements. These are used to online measure the field distribution with optical magnetometers and the fluctuations of gradients *e.g.* with SQUIDs. By performing two Ramsey experiments simultaneously in two chambers with inverted E-fields in the same magnetic field, drifts of the homogeneous B_0-field are canceled, only fluctuations in the vertical gradient affect the measurement. Gradients are extracted from four stacked ^{199}Hg cells, similar to ref. [20] with an accuracy of $< 10\,\mathrm{fT}$. The measurement contains effects that shift the frequencies of both species in different ways and thus mimic a false EDM signal as well as effects that increase the error bar on the measured result without applying a shift in frequency. The analysis of the measurement is conceptually based on the Sussex-RAL-ILL experiment with a double magnetometer [13]. The velocities of UCN and ^{199}Hg differ significantly, thus the average center of gravity is $\Delta h \sim 2.5\,\mathrm{mm}$ lower for UCN. Therefore, a vertical gradient changes the ratio R of the spin precession frequencies of both species in a chamber.

2˙1. *Systematic effects.* – Generally, any systematic effects can be classified as i) directly magnetic field related, mainly drifts and fluctuations of gradients, as well as leakage currents; ii) particle motion related effects, like geometric phases of the Hg atoms and the neutrons in *e.g.* B and E inhomogeneities and iii) mechanical effects, like vibrations, alignment of electrodes or laser beams, symmetry of the chamber and shutters. Magnetic fields and gradient drifts between the chamber positions can be controlled already with ^{199}Hg magnetometry to a level of 10 fT, which represents about the minimum accuracy for a maximum allowed false EDM of $d_{\mathrm{false}} \sim 1 \cdot 10^{-28}\,\mathrm{ecm}$ in case of merely statistical magnetic field fluctuations. The homogeneity of the residual fields and the generated fields is practically limited to $< 0.3\,\mathrm{nT/m}$ gradients over the volume of the chambers and magnetometers. A combination with the motional magnetic field of a particle moving in an electric field gives rise to a term

$$\delta\omega \sim \frac{\partial B}{\partial z} r \left(\vec{E} \times \vec{v}\right), \tag{4}$$

linear with E, the so-called geometric phase effect. Due to the larger velocities of the Hg atoms, this effect amounts to $d_{\mathrm{false}} \sim 4 \cdot 10^{-27}\,\mathrm{ecm}$ for a current generation Hg magnetometer and $d_{\mathrm{false}} \sim 2 \cdot 10^{-28}\,\mathrm{ecm}$ for the neutrons. In addition to the requirements

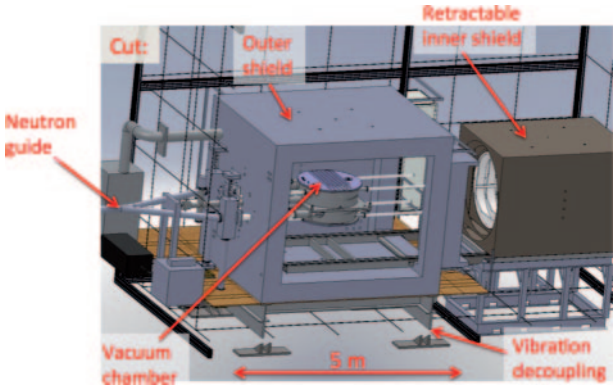

Fig. 2. – Cut through the EDM installation with retracted innermost shields.

on the overall B_0 field, this also severely constrains magnetic contaminations to pT within few cm close to the neutron chambers and *e.g.* light shifts from the readout light of the ^{199}Hg magnetometers. As deduced from simulations, also *e.g.* the alignment of E and B_0 must be controlled to 10^{-4}, vibrations also are critical and are controlled via laser interferometry. Fluctuations of the high voltage also cause non-negligible currents that are avoided with a fully non-metallic layout, which also helps to avoid the introduction of RF noise from outside through the HV conductor. Whereas the velocity of Hg atoms is fixed in such a scheme, the UCN velocities can be changed without changing any parameters inside the spectrometer. This is done deploying a superconducting solenoid along the neutron guide that supplies UCN to the EDM spectrometer. In the center of the solenoid, a resonant spin flipper is operated. The field strength can be adjusted within a range of values while keeping the spin flipper resonant. This splits the initial UCN spectrum from the solid deuterium based source with a minimum kinetic energy of 108 neV into a fast and a slow polarized spectrum with tunable energy (see, *e.g.* ref. [21]). While the slow spin component is stored in the EDM chambers, the accelerated polarization will not be trapped due to the high kinetic energy.

2˙2. *Magnetic environment.* – The EDM spectrometer is placed in a non-magnetic building outside the reactor. This yields several advantages for the performance of the experiment: the floor is magnetically and vibrationally decoupled and built with low magnetism materials on an area of $6 \times 9\,\mathrm{m}^2$, covered by a temperature and humidity controlled clean-room environment. An active 24 coil ambient field compensation coil system with 180 magnetic field probes is used to compensate for static and dynamic ambient fields and second order gradients. Passive shielding made from Mu-metal and aluminum shells in a nested cuboid arrangement then reduce electromagnetic disturbances at different ranges of frequencies. The passive shield is split in an outer shielded room on a vibration controlled table with a large access door and a 1 nT residual field inside. Already in this environment, the EDM spectrometer can be assembled and tested with easy access. On a rail system, an inner magnetic shield section can slide into the room. This inner shield section is again built up from cuboid Mu-metal parts, with detachable end-caps. A cylindrical Mu-metal shield with $\sim$ 1.5 m diameter forms the innermost layer inside this cuboid assembly. This cylinder is optimized to interact with the coils required for the B_0 field, as well as for demagnetization. An overview picture of the installation is shown in fig. 2. The shielded room with all integrated systems is

portable, it can be lifted by crane and transported by truck in one piece. In particular, it rests on a table that can be adjusted in height to modify the energy distribution of UCN inside the EDM chambers.

2˙3. *Schedule*. – The construction work for the beam position, installation of clean rooms, compensation system and outer magnetic shielding is ongoing. Subsequently, the installation of magnetometry systems and the inner magnetic environment is scheduled in 2012, after finalizing ongoing tests of a small scale prototype.

* * *

This work is supported by the Deutsche Forschungsgemeinschaft (SPP 1491) and the DFG cluster of excellence Origin and Structure of the Universe.

REFERENCES

[1] Purcell E. M. and Ramsey N. F., *Phys. Rev.*, **78** (1950) 807.
[2] Barr S. M., *Int. J. Mod. Phys. A*, **8** (1993) 209.
[3] Christenson J. H., Cronin J. W., Fitch V. L. and Turlay R., *Phys. Rev. Lett.*, **13** (1964) 138.
[4] Aubert B. *et al.*, *Phys. Rev. Lett.*, **86** (2001) 2515.
[5] Kobayashi M. and Maskawa K., *Prog. Theor. Phys.*, **49** (1973) 652.
[6] Barbieri R., *Nucl. Phys. B*, **449** (1995) 437.
[7] Bigi I. I. and Sanda A. I., *CP Violation* (Cambridge University Press, UK) 2000.
[8] Riotto A. and Trodden M., *Annu. Rev. Nucl. Sci.*, **49** (1999) 35.
[9] Sakharov A. D., *JETP Lett.*, **5** (1967) 24.
[10] Ramsey N. F., *Rep. Prog. Phys.*, **45** (1982) 95.
[11] He X., McKellar B. H. and Paskvasa S., *Int. J. Mod. Phys. A*, **4** (1989) 5011.
[12] Pospelov M. and Ritz A., *Ann. Phys.*, **318** (2005) 119.
[13] Baker C. A, Doyle D. D., Geltenbort P., Green K. *et al.*, *Phys. Rev. Lett.*, **97** (2006) 131801.
[14] Hudson J. J. *et al.*, *Nature*, **473** (2011) 494.
[15] Griffith W. C., Swallows M. D., Loftus T. H., Romalis M. V., Heckel B. R. and Fortson E. N., *Phys. Rev. Lett.*, **102** (2009) 101601.
[16] Frei A. *et al.*, *Eur. Phys. J. A*, **34** (2007) 119.
[17] Frei A. *et al.*, *EPL*, **92** (2010) 62001.
[18] Frei A. *et al.*, *Nucl. Instrum. Methods A*, **612** (2010) 349.
[19] HG und laser, *Phys. Rev. Lett.*, **102** (2009) 101601.
[20] Jacobs J. P., Klipstein W. M., Lamoreaux S. K., Heckel B. R. *et al.*, *Phys. Rev. A*, **52** (1995) 5.
[21] Rauch H. and Alefeld B., *Z. Phys. B*, **41** (1981) 231.